

Statistical analysis and modeling of variations of the earth's magnetic field

Jon D. Pelletier

Department of Geological Sciences, Snee Hall, Cornell University

Ithaca, NY 14853

Power spectral analyses of the dipole moment of the earth's magnetic field inferred from ocean sediment cores and archeomagnetic data from time scales of 100 yr to 4 Myr have been carried out. The power spectrum is proportional to $1/f$ where f is the frequency. These analyses compliment previous work which has established a $1/f^2$ spectrum for variations at time scales less than 100 yr. Power spectral analyses of inclination and declination inferred from lake sediments from time scales of 10 yr to 30 kyr have also been performed. The spectra are constant above time scales of 3 kyr, proportional to $1/f^2$ from time scales of 500 yr to 3 kyr, and constant again below time scales of 500 yr. The 3 kyr time scale is associated with the decay time of the quadrupole moment. We test the hypothesis that reversals are the result of variations in dipole intensity with a $1/f$ spectrum which occasionally are large enough to cross the zero intensity value. Synthetic binormal time series with a $1/f$ power spectrum representing variations in the earth's dipole moment are constructed. Synthetic reversals from these time series exhibit statistics in good agreement with the reversal record. $1/f$ noise behavior is reproduced with a model of magnetic diffusion in the earth's core driven by dynamo action modeled as a random amplification or destruction of the local magnetic field.

I. INTRODUCTION

The earth's magnetic field has exhibited significant variability over a wide range of time scales. On time scales less than a couple of hundred years historical data are available for variations in the intensity and orientation of the geomagnetic field. Archeomagnetic data can be used to infer the intensity of the field from time scales of centuries to millenia. Sediment cores provide the widest range of time scales of variations in the geomagnetic field with internal origin: 1 kyr to several Myr. Techniques of time series analysis can be used to characterize this variability. The power spectrum is the square of the coefficients of the Fourier transform of the time series. It quantifies the average variability of the series at different time scales. Barton (1982) has performed spectral analysis of paleointensity using historical observations and sediment cores. He identified a broad, continuous power spectrum with a steep dependence on time scale for time scales less than a century and a flatter spectrum at longer time scales.

The geomagnetic field also exhibits reversals with a complex history including variations over a wide range of time scales. The reversal history can be characterized by the polarity interval distribution and the reversal rate. Polarity intervals vary from those short enough to be barely resolved in the magnetic anomalies of the seafloor to the 35 Myr Cretaceous superchron. Reversals are also clustered in time such that short polarity intervals tend to be followed by short polarity intervals and long intervals by long intervals. This clustering has been quantified with the reversal rate which gradually decreases going back to 100 Ma and then increases going back further in time before the Cretaceous superchron.

Due to the availability of many new time series data sets for paleointensity and inclination and declination of the earth's magnetic field since the work of Barton (1982), it would be useful to perform power spectral analyses of some of these recent data sets to further characterize the temporal variability of the geomagnetic field. In this paper we perform power spectral analyses of time series data for the dipole moment and the inclination and declination of the earth's magnetic field inferred from sediment core and archeomagnetic

data. We find that the power spectrum of the virtual axial dipole moment (VADM) from time scales of 100 yr to 4 Myr is well approximated by a $1/f$ dependence, where f is the frequency. The power spectrum of inclination and declination are constant above time scales of 3 kyr, proportional to $1/f^2$ from time scales of 500 yr to 3 kyr, and constant again below time scales of 500 yr. Variations in the intensity of the geomagnetic field in one polarity exhibits a normal distribution. When a fluctuation crosses the zero intensity value a reversal occurs. We test the hypothesis that reversals are the result of intensity variations with a $1/f$ power spectrum which occasionally are large enough to cross the zero intensity value, driving the geodynamo into the opposite polarity state. Synthetic time series with a $1/f$ power spectrum and a binormal distribution are used to generate reversal statistics. These are found to be in good agreement with those of the real reversal history. The reversal statistics are sensitive to the form of the power spectrum of intensity variations. We conclude that the agreement between the synthetic reversal record produced with $1/f$ noise variations in the earth's dipole moment is strong support for $1/f$ behavior over the length of the reversal record. This suggests that processes internal to the core may determine geomagnetic variability up to very long time scales. This contrasts with the hypothesis that internal core processes dominate secular variations while changes in conditions at the core-mantle boundary determine variations at larger time scales (McFadden and Merrill, 1995). A model of geomagnetic variability based on internal processes of magnetic diffusion and dynamo action modeled as a stochastic process generates the observed $1/f$ behavior. This model is analyzed in detail and compared to the behavior of the earth's magnetic field.

II. POWER SPECTRAL ANALYSES OF THE VIRTUAL AXIAL DIPOLE MOMENT

Paleomagnetic studies clearly show that the polarity of the magnetic field has been subject to reversals. Kono (1971) has compiled paleointensity measurements of the magnetic field from volcanic lavas for 0-10 Ma. He concluded that the distribution of paleointensity

is well approximated by a symmetric binormal distribution with mean $8.9 \times 10^{22} \text{Am}^2$ and standard deviation $3.4 \times 10^{22} \text{Am}^2$. One normal distribution is applicable to the field when it is in its normal polarity and the other when it is in its reversed polarity.

We have utilized three datasets for computing the power spectrum of the dipole moment of the earth's magnetic field. They are archeomagnetic data from time scales of 100 yr to 8 kyr from Kovacheva (1980), marine sediment data from the Somali basin from time scales of 1 kyr to 140 kyr from Meynadier et al. (1992), and marine sediment data from the Pacific and Indian Oceans from 20 kyr to 4 Myr from Meynadier et al. (1994). The data were published in table form in Kovacheva (1980) and obtained from L. Meynadier (Meynadier, 1995) for the marine sediment data in Meynadier et al. (1992) and Meynadier et al. (1994). Marine sediment data are accurate measures of relative paleointensity but give no information on absolute intensity. In order to calibrate marine sediment data, the data must be compared to absolute paleointensity measurements from volcanic lavas sampled from the same time period as the sediment record. Meynadier et al. (1994) has done this for the composite Pacific and Indian Ocean dataset. They have calibrated the mean paleointensity in terms of the virtual axial dipole moment for 0-4 Ma as $9 \times 10^{22} \text{Am}^2$ (Valet and Meynadier, 1993). This value is consistent with that obtained by Kono (1971) for the longer time interval up to 10 Ma. Using this calibration, we calibrated the Somali data with the time interval 0-140 ka from the composite Pacific and Indian Ocean dataset. The data from Meynadier et al. (1994) are plotted in Figure 1 as a function of age in Ma. The last reversal at approximately 730 ka is clearly shown. We computed the power spectrum of each of the time series with the Lomb periodogram (Press et al., 1992). The compiled spectra are given in Figure 2. The composite sediment record from the Pacific and Indian Oceans are plotted up to a frequency corresponding to a period of 25 kyr. Above this time scale good synchronicity is observed in the Pacific and Indian Ocean datasets (Meynadier et al., 1994). This suggests that non-geomagnetic effects such as variable sedimentation rate are not significant in these cores above this time scale. From frequencies corresponding to time scales of 25 kyr down to 1.6 kyr we plot the power spectrum of the Somali data. From time scales of 1.6 kyr to

the highest frequency we plot the power spectrum of the data of Kovacheva (1980). A least-squares linear regression to the data yields a slope of -1.09 over 4.5 orders of magnitude. This indicates that the power spectrum is well approximated as $1/f$ on these time scales.

The power spectrum of secular geomagnetic intensity variations has been determined to have a $1/f^2$ power spectrum between time scales of one and one hundred years (Currie, 1968; Barton, 1982; Courtillot and Le Mouel, 1988). This is consistent with the analysis of McLeod (1992) who found that the first difference of annual means of geomagnetic field intensity is a white noise since the first differences of a random process with power spectrum $1/f^2$ is a white noise. Our observation of $1/f$ power spectral behavior above time scales of approximately 100 yr together with the results of Currie (1968) and Barton (1982) suggests that there is a crossover from $1/f$ to $1/f^2$ spectral behavior at a time scale of approximately one hundred years.

III. ANALYSIS OF THE REVERSAL HISTORY

In this section we will test the hypothesis that reversals are the result of intensity variations in one polarity state becoming large enough to cross the zero intensity value into the opposite polarity state. We will show that the statistics of the reversal record are consistent those of a binormal, $1/f$ noise paleointensity record which reverses when the intensity crosses the zero value. We will compare the polarity length distribution and the clustering of reversals between synthetic reversals produced with $1/f$ noise intensity variations and the reversal history according to Harland et al. (1990) and Cande and Kent (1992a,1995).

First we consider the polarity length distribution of the real reversal history. The polarity length distribution calculated from the chronology of Harland et al. (1990) is given as the solid line in Figure 3. The polarity length distribution is the number of interval lengths longer than the length plotted on the horizontal axis. A reassessment of the magnetic anomaly data has been performed by Cande and Kent (1992a,1995) to obtain an alternative magnetic time scale. Their chronology, normalized to the same length as the Harland et

al. (1990) time scale, is presented as the dashed curve. The two distributions are nearly identical. These plots suggest that the polarity length distribution is better fit by a power law for large polarity lengths than by an exponential distribution, as first suggested by Cox (1968). The same conclusion has been reached by Gaffin (1989) and Seki and Ito (1993). It should be emphasized, however, that the polarity length distribution is a very different analysis than that of the spectral analysis of Section 2. There is no simple relationship between the power spectrum of intensity variations and the polarity length distribution of reversals. The observation of a power-law power spectrum in Section 2 does not necessarily imply a power-law polarity length distribution.

The third curve, plotted with a dashed and dotted line, represents the polarity length distribution estimated from the magnetic time scale between C1 and C13 with “cryptochrons” included and scaled to the length of the Harland et al. (1990) time scale. Cryptochrons are small variations recorded in the magnetic anomaly data that may either represent variations in paleomagnetic intensity or short reversals (Blakely, 1974; Cande and Kent, 1992b). Cryptochrons occur with a time scale at the limit of temporal resolution of the reversal record from magnetic anomalies of the sea floor. The form of the polarity length distribution estimated from the record between C1 and C13 including cryptochrons is not representative of the entire reversal history because of the variable reversal rate which concentrates many short polarity intervals in this time period. However, this distribution enables us to estimate the temporal resolution of the reversal record history. The distribution estimated from C1 to C13 has many more short polarity intervals than those of the full reversal history starting at a reversal length of 0.3 Myr. Above a time scale of 0.3 Myr the magnetic time scale is nearly complete. Below it many short polarity intervals may be unrecorded.

To show that the polarity length distribution of the real reversal record is consistent with that produced by binormal, $1/f$ noise variations in the earth’s dipole moment, we have generated synthetic Gaussian noises with a power spectrum proportional to $1/f$, a mean value of $8.9 \times 10^{22} \text{Am}^2$ and a standard deviation of $3.4 \times 10^{22} \text{Am}^2$. These synthetic noises represent the field intensity in one polarity state. The synthetic noises were generated using

the Fourier-domain filtering technique described in Turcotte (1992). An example is shown in Figure 4a. In order to construct a binormal intensity distribution from the synthetic normal distribution, we inverted every other polarity interval to the opposite polarity starting from its minimum value below the zero intensity axis and extending to its next minimum below the zero. The result of this procedure on the Gaussian, $1/f$ noise of Figure 4a is presented in Figure 4b. Its irregular polarity lengths are similar to those in the marine sediment data of Figure 1.

The operation of reversing the paleomagnetic intensity when it crosses the zero intensity value is consistent with models of the geodynamo as a system with two symmetric attracting states of positive and negative polarity such as the Rikitake disk dynamo (Rikitake, 1958). Between reversals, the geomagnetic field fluctuates until a fluctuation large enough occurs to cross the energy barrier into the other basin of attraction. Kono (1987) has explored the statistical similarity between the Rikitake disk dynamo and the distribution of paleointensity. Our construction of the binormal $1/f$ noise is consistent with this model.

We have computed the distribution of lengths between successive reversals for twenty synthetic noises scaled to 170 Ma, the length of the reversal chronology, and averaged the results in terms of the number of reversals. The results are given in Figure 5. The dots are the maximum and minimum values obtained in the twenty synthetic reversal chronologies, thus representing 95% confidence intervals. The polarity interval distribution from the Harland et al. (1990) time scale indicated by the dashed curve falls within the 95% confidence intervals of our synthetic data over all time scales plotted except for the Cretaceous superchron, which lies slightly outside of the 95% confidence interval and reversals separated by less than about 0.3 Myr. The overprediction of very short reversals could be a limitation of the model or a result of the incompleteness of the reversal record for short polarity intervals. As mentioned, the temporal resolution of the magnetic time scale inferred from magnetic anomalies is approximately 0.3 Myr. We conclude that the polarity length distribution produced from binormal $1/f$ intensity variations are consistent with the observed polarity length distribution for all time scales at which the reversal record is complete.

We next consider whether the agreement illustrated in Figure 5 is unique to $1/f$ noise. We have computed polarity length distributions using the binormal intensity variations with power spectra $f^{-0.8}$ and $f^{-1.2}$. These results along with the $1/f$ result from Figure 5 are given in Figure 6. The shape of the polarity length distribution is very sensitive to the exponent of the power spectrum. A slight increase in the magnitude of the exponent results in many more long polarity intervals than with $1/f$ noise. We conclude that the agreement in Figure 5 between the synthetic reversal distribution and the true reversal history is unique to $1/f$ noise and provides strong evidence that the dipole moment has $1/f$ behavior up to 170 Ma.

A binormal, $1/f$ noise geomagnetic field variation is consistent with the qualitative results of Pal and Roberts (1988) who found an anticorrelation between reversal frequency and paleointensity. This anticorrelation is evident in the synthetic $1/f$ noise of Figure 4b. During the time intervals of greatest average paleointensity the reversal rate is lowest.

In addition to the broad distribution of polarity lengths, the reversal history is also characterized by a clustering of reversals. This behavior has been quantified with the reversal rate. The reversal rate has been relatively high from 0-20 Ma and has decreased gradually going back in history to the Cretaceous superchron. An alternative approach to quantifying the clustering of reversals is with the pair correlation function. The pair correlation function $c(t)$ is the number of pairs of reversals whose separation is between t and $t + \Delta t$, per unit time (Vicsek, 1992). The pair correlation function for a set of points can be compared to that for a Poisson process to detect non-random clustering. The pair-correlation function analysis is more appropriate for comparison of the reversal history to the synthetic reversal history generated by a stochastic model such as model based on turbulent processes in the core. This is because stochastic models cannot predict behavior in time, such as when the reversal rate is large or small. However, a stochastic model may accurately reflect the extent to which small polarity intervals are followed by small polarity intervals and long intervals by long intervals as quantified with the pair correlation function.

The pair correlation function of reversals according to the Harland et al. (1990) and

Cande and Kent (1992a,1995) reversal history are shown in Figure 7 as filled and unfilled circles, respectively. Also presented in Figure 7 is the pair correlation function for a synthetic reversal data set based on binormal $1/f$ noise dipole moment variations (boxes) and the pair correlation function for a Poisson process (triangles). The functions are offset so that they may be placed on the same graph. The Poisson process was constructed with 293 points, the same number of reversals as the Harland et al. (1990) time scale, positioned with uniform probability on the interval between 0 and 170 Ma. The Poisson process yields a correlation function independent of separation. The real and synthetic reversal histories variations exhibit significant clustering with more pairs of points at small separation and fewer at large separations than for a Poisson process. Straight-line fits of the form $c(t) \propto t^\alpha$ were obtained. The purpose of this was to show that similar clustering is observed in the real and synthetic reversals. The exponents α of the Harland et al. (1990), Cande and Kent (1992a,1995), and synthetic reversals are -0.39, -0.31, and -0.42, respectively. Similar non-random clustering is observed in the real and synthetic reversals. We conclude from the consistency between the polarity interval distribution and pair correlation function of real reversals and those generated by fluctuations of a binormal $1/f$ noise process that there is strong evidence for $1/f$ intensity variations for time scales up to the length of the reversal record.

IV. POWER SPECTRAL ANALYSES OF INCLINATION AND DECLINATION

Power spectral analyses of inclination and declination data have also been carried out. We obtained time series data of inclination and declination from lake sediment cores in the Global Paleomagnetic Database (Lock and McElhinney, 1992). The core with the greatest number of data points was from Lac du Bouchet (Thouveny et al., 1990). The power spectrum of the inclination and declination at Lac du Bouchet estimated with the Lomb Periodogram is presented in Figure 8. We associate the spectra with a constant spectrum below a frequency of $f \approx 1/(3 \text{ kyr})$ and a constant spectrum above a frequency of $f \approx$

1/(500 yr). From frequencies of $f \approx 1/(3 \text{ kyr})$ to $f \approx 1/(500 \text{ yr})$ the inclination and declination are Brownian walks with $S(f) \propto f^{-2}$. Spectral analyses of inclination data from five other sediment cores were calculated. These spectra are presented in Figure 9. The spectra correspond, from top to bottom, to cores from Anderson Pond (Lund and Banerjee, 1985), Bessette Creek (Turner et al., 1982), Fish Lake (Verosub et al., 1986), Lake Bullenmerri (Turner and Thompson, 1981), and Lake Keilambete (Barton and McElhinny, 1985). Since the data sets have fewer points there is more uncertainty in the spectra and they are characterized by greater variability between adjacent frequencies. The spectra have the same form, within the uncertainty of the spectra, as that associated with the spectra from Lac du Bouchet. These results suggest that 3 kyr and 500 yr are characteristic time scales of geodynamo behavior. Variations in inclination and declination are associated with changes in the non-dipole components of the field. Therefore, the autocorrelation or decay time of the quadrupole moment is the maximum time scale for correlated fluctuations of inclination and declination to occur. The autocorrelation time of the quadrupole moment has been estimated by McLeod (1996) to be 1.6 kyr. This is within a factor of two of the 3 kyr time scale above which variations in inclination and declination are observed to be uncorrelated in the spectra of Figures 8 and 9.

Many analyses of variations in paleointensity of the earth’s magnetic field concentrate on identifying characteristic time scales of variation. Many such characteristic time scales have been identified. Valet and Meynadier (1993) suggested, based on the same sediment core data analyzed in this paper, that the earth’s magnetic field regenerates following a reversal on a time scale of a few thousand years and then decays slowly on a time scale of 0.5 Ma before the next reversal. They termed this an “asymmetric saw-tooth” pattern. More recent data have shown that the “asymmetric saw-tooth” is not a robust pattern. Longer cores show a slow decay preceding a reversal to be rare (Tauxe and Hartl, 1997). Moreover, Laj et al. (1996) has shown that the magnetic field does not always regenerate quickly after a reversal. Thibault et al. (1995) have quantified the rate of decrease in field intensity preceding a reversal and found it to be inversely proportional to the length of

the polarity interval. The authors concluded from this that the length of the reversal was predetermined. Such behavior is not indicative of a predetermined polarity length. This can be concluded by considering the null hypothesis that variations in the field are characterized by any stationary random process. By definition, a stationary time series has a variance which is independent of the length of the series. The average rate of change of the time series over a time interval will then be a constant value divided by the interval of time, i.e. inversely proportional to time interval. Therefore, any stationary random function satisfies the relationship that Thibault et al. (1995) observed.

In the power spectral analyses of geomagnetic variations inferred from sediment cores by Lund et al. (1988), Meynadier et al. (1992), Lehman et al. (1996), and Tauxe and Hartl (1997) dominant periodicities in the record were identified and proposed as characteristic time scales of geodynamo behavior. However, it must be emphasized that any finite length record will exhibit peaks in its power spectrum, even if the underlying process is random, such as a $1/f$ noise. Periodicity tests such as those developed by Lees and Park (1995) need to be applied to data in order to assess the probability that a peak in a spectrum is statistically significant. The periodicity tests developed by Lees and Park (1995) are especially valuable because they do not depend on a particular model of the stochastic portion of the spectrum. Some of the periodicity tests that have been used in the geomagnetism literature assume forms for the stochastic portion of the spectrum that are not compatible with the $1/f$ process we have identified. See Mann and Lees (1996) for an application of these techniques to climatic time series.

It is generally believed that secular geomagnetic variations are the result of internal dynamics while longer time scale phenomena such as variations in the reversal rate are controlled by variations in boundary conditions at the core-mantle boundary (CMB) (McFadden and Merrill, 1995). However, our observation of continuous $1/f$ spectral behavior from time scales of 100 yr to 170 Myr suggests that a single process controls variations in geomagnetic intensity over this range of time scales. In Section 6 we consider a model for geodynamo behavior which reproduces the $1/f$ dipole moment variations over a wide range

of time scales and exhibits many of the other features of geomagnetic variability we have identified.

V. MULTIPOLE EXPANSION OF THE PRESENT DAY GEOMAGNETIC FIELD

In addition to temporal variations of the field, detailed information on the spatial structure of the present-day magnetic field from spherical harmonic degree $n = 1$ to $n = 13$ is available. Above $n = 13$ the magnetic field at the earth's surface is dominated by crustal magnetic fields. Stevenson (1983) and Voorhies and Conrad (1996) have presented the results of a spherical harmonic expansion of the geomagnetic field extrapolated to the core-mantle boundary. The results indicate that a broad spectrum of multipoles is represented with an intensity decreasing with increasing order in the spherical harmonic expansion. The spectrum is consistent with a power-law function of wave number at the core-mantle boundary with exponent -1 : $R_n \propto n^{-1}$. The form of the spectrum is not well constrained since an exponential fit, first proposed by Langel and Estes (1982), and a power-law fit both match the observed spectrum equally well from $n = 1$ to $n = 13$. This is illustrated in Figure 1 of McLeod (1996) where the two fits are compared. Although the data does not allow an unambiguous determination of the functional form of the spectrum, Stevenson (1983) has shown that a spectrum $R_n \propto n^{-1}$ is consistent with a multipole expansion expected based upon other considerations. Stevenson argues that an exponent close to -1 is the only one consistent with energy conservation given the typical convective velocities and the magnetic Reynolds number expected in terrestrial dynamos. Voorhies and Conrad (1996) have argued that a $R_n \propto n^{-1}$ amplitude spectrum at the core-mantle boundary does a superior job at predicting the location of the core-mantle boundary and provides a better extrapolation to the observed dipole field. In the next section we discuss a model of the earth's magnetic field which generates a field with a power spectrum $R_n \propto n^{-1}$.

VI. MODELING OF VARIATIONS IN THE EARTH'S MAGNETIC FIELD BY DYNAMO PROCESSES

There has been great interest in $1/f$ noise processes in the physics literature for many years (Weissman, 1988). One model of $1/f$ noise is a stochastic process comprised of a superposition of modes with exponential decay characterized by different time constants. The time constant for a stochastic process is defined through its autocorrelation function $a(\tau)$. For a stochastic process with a single time constant τ_o the autocorrelation function is given by $a(\tau) = e^{-\frac{\tau}{\tau_o}}$. The power spectrum of such a process is, by the Weiner-Khinchine theorem, the Fourier transform of the autocorrelation function:

$$S(f) \propto \frac{\tau_o}{1 + (2\pi f)^2} \quad (1)$$

This is a Lorentzian spectrum with Brownian walk behavior ($S(f) \propto f^{-2}$) for time scales small compared to τ_o and white noise behavior ($S(f) = \text{constant}$) above the characteristic time constant. If the stochastic process is composed of a superposition of modes with time constants following a distribution $D(\tau_o) \propto \tau_o^{-1}$, where the $D(\tau_o)\Delta\tau_o$ is the net variance contributed by modes between τ_o and $\tau_o + \Delta\tau_o$, then a $1/f$ spectrum results over a range of frequencies (van der Ziel, 1950; Weissman, 1988). Such a distribution of exponential time constants has been documented for the earth's magnetic field by McLeod (1996).

McLeod (1996) calculated the autocorrelation of each degree of the geomagnetic field during the last eighty years. The autocorrelation functions that he computed had an exponential dependence on time with degree-dependent time constants $\tau_o \propto n^{-2}$. This behavior is consistent with a diffusion process. McLeod (1996) attributed this autocorrelation structure to a simple model of the geomagnetic field in which the field was stochastically generated with a balance between field regeneration and diffusive decay by decay across a magnetic boundary layer. One way to model such a stochastic diffusion process is with a two-dimensional diffusion equation driven by random noise:

$$\frac{\partial B_z}{\partial t} = D\nabla^2 B_z + \eta(x, y, t) \quad (2)$$

where B_z is the axial component of the magnetic field at a point inside the core, $\eta(x, y, t)$ is a Gaussian white noise representing random amplification and destruction of the field locally by dynamo action. To this equation we add a term equal to $p - B_{z,tot}$:

$$\frac{\partial B_z}{\partial t} = D\nabla^2 B_z + \eta(x, y, t) + c(p - B_{z,tot}) \quad (3)$$

where c is a constant, $B_{z,tot}$ is the dipole moment integrated over all space, and p is +1 if the dipole moment of the field outside the core-mantle boundary is positive and -1 if the dipole moment outside the core-mantle boundary is negative. The effect of this term is to create two basins of attraction (polarity states) within which the dipole field fluctuates around an intensity of +1 or -1 until a fluctuation large enough occurs to cross the barrier to the other basin of attraction. This term could be the result of a conservation of magnetic energy for the combination of the poloidal and toroidal fields such that when the poloidal dipole field intensity is low the toroidal field intensity, which is unobservable outside the core and not explicitly modeled in equation 3, is high and dynamo action is intensified, repelling the poloidal field away from a state of low dipole intensity.

In our model the core is modeled as a two-dimensional circular region of uniform diffusivity (the fluid outer core) surrounded by an infinite region with small but finite diffusivity and the boundary condition that B_z approach zero as r , the radial distance from the center of the earth, approaches infinity. The diameter of the inner circular region is the diameter of the core-mantle boundary.

This model has been studied in terms of the distribution of values and power spectrum of the dipole moment and the power spectrum of the angular deviation from the dipole field. The dipole field from the simulation is plotted in Figure 10. The field clearly undergoes reversals with a broad distribution of polarity interval lengths. Figure 11 presents the dipole distribution of 10 simulations (solid curve) along with the fit to a binormal distribution (dashed curve). A binormal distribution fits the distribution well. The slight asymmetry is the result of this particular model run spending slightly more time in the negative polarity state than the positive polarity state. Model outputs were generated which showed

asymmetry in the other direction.

The average power spectrum of time series of the dipole field from 25 simulations is presented in Figure 12. The spectrum has a low-frequency spectrum $S(f) \propto f^{-1}$ and a high-frequency spectrum $S(f) \propto f^{-2}$. This is identical to the spectrum observed in sediment cores and historical data discussed in Section 2. The crossover time scale is the diffusion time across the diameter of the core, estimated to be between 10^3 (Harrison and Huang, 1990) and 10^4 yr (McLeod, 1996). These values are somewhat higher than the order of magnitude time scale of 10^2 yr identified as the crossover in the sediment core and historical data. The average power spectrum of the angular deviation from the dipole from 25 simulations is shown in Figure 13. The spectrum has a high-frequency region $S(f) \propto f^{-2}$ which slowly flattens out to a constant spectrum at low frequencies. This is nearly consistent with the spectra of inclination and declination from lake sediment time series shown in Figures 8 and 9. The $S(f) \propto f^{-2}$ begins to flatten out at a time scale roughly equivalent to the time scale of the intensity spectrum to cross over from $1/f$ to $1/f^2$ behavior. The measured value of this crossover in the lake sediment power spectra is 3 kyr. This value is consistent with estimates of 10^3 to 10^4 years for the diffusion time across the core from Harrison and Huang (1990) and McLeod (1996). A major discrepancy between the model and the observed spectra is the absence of a flattening out of the spectrum at high frequencies in the model calculation.

The average spatial power spectrum of transects of B_z for 25 simulations is given in Figure 14. The spectrum is $S(k) \propto k^{-1}$. This is consistent with the $R_n \propto n^{-1}$ power spectrum from a spherical harmonic expansion as observed for the spatial power spectrum of the earth's magnetic field. The power spectrum of one-dimensional transects is directly comparable to the power spectrum from a spherical harmonic expansion. For example, the power spectrum of the earth's topography and bathymetry has been estimated from Fourier analysis of one-dimensional transects and from a spherical harmonic expansion. The spectral exponents obtained are identical in the two analyses (Turcotte, 1992).

Although this model reproduces many of the observed features of the variability of the

earth's magnetic field, the physical origin of the terms in the model equation have not been specified. Gaussian white noise amplification and decay of the magnetic field by dynamo action is a simple stochastic model for dynamo action but there is no physical justification for it. Moreover, we have presented no clear physical justification for the term $p - B_{z,tot}$ which generates field reversals and a binormal distribution of dipole intensity. These terms were included in the model in order to construct a minimal model consistent with the complex behavior of the earth's magnetic field.

VII. CONCLUSIONS

We have presented the results of power spectral analyses of variations in the dipole moment of the earth's magnetic field which show the spectrum to be proportional to $1/f$ from time scales of 100 yr to 4 Myr. We have also performed spectral analyses of variations in inclination and declination. These spectra are constant above time scales of 3 kyr, proportional to $1/f^2$ from time scales of 500 yr to 3 kyr, and constant again below time scales of 500 yr. The 3 kyr time scale is associated with the decay time of the quadrupole moment. We have shown that reversals generated by binormal, $1/f$ noise geomagnetic field intensity variations are consistent with the distribution of polarity lengths and clustering of real reversals. We have shown how a model of magnetic diffusion driven by dynamo action parameterized as a stochastic process reproduces many of the observed features of the spatial and temporal variability of the earth's magnetic field.

ACKNOWLEDGMENTS

We wish to thank Donald L. Turcotte for helpful conversations and Laure Meynadier for access to the marine sediment data and helpful conversations regarding its interpretation.

Barton, C.E., Spectral analysis of palaeomagnetic time series and the geomagnetic spectrum, *Phil. Trans. R. Soc. London A*, **306**, 203-209, 1982.

Blakely, R.J., Geomagnetic reversals and crustal spreading rates during the Miocene, *J. Geophys. Res.*, **79**, 2979-2985, 1974.

Cande, S.C. and Kent, D.V., A new geomagnetic polarity time scale for the Late Cretaceous and Cenozoic, *J. Geophys. Res.*, **97**, 13,917-13,951, 1992a.

Cande, S.C. and Kent, D.V., Ultrahigh resolution marine magnetic anomaly profiles : a record of continuous paleointensity variations?, *J. Geophys. Res.*, **97**, 15075-15083, 1992b.

Cande, S.C. and Kent, D.V., Revised calibration of the geomagnetic polarity timescale for the Late Cretaceous and Cenozoic, *J. Geophys. Res.*, **100**, 6093-6095, 1995.

Courtillot, V. and Le Mouél, J.L., Time variations of the earth's magnetic field: From daily to secular, *Ann. Rev. Earth Plan. Sci.*, **16**, 389-476, 1988.

Cox, A., Lengths of geomagnetic polarity intervals, *J. Geophys. Res.*, **73**, 3247-3260, 1968.

Currie, R.G., Geomagnetic spectrum of internal origin and lower mantle conductivity, *J. Geophys. Res.*, **73**, 2779-2768, 1968.

Gaffin, S., Analysis of scaling in the geomagnetic polarity reversal record, *Phys. Earth Plan. Inter.*, **57**, 284-290, 1989.

Harland, W.B., Cox, A., Llewellyn, P.G., Pickton, C.A.G., Smith, A.G., and Walters, R., 1990. *A Geologic Time Scale 1989*, Cambridge University Press, London, 1989.

Harrison, C.G.A. and Huang, Q., Rates of change of the Earth's magnetic field measured by recent analyses, *J. Geomag. Geoelectr.*, **42**, 897-928, 1990.

Kono, M., Intensity of the earth's magnetic field during the Pliocene and Pleistocene in relation to the amplitude of mid-ocean ridge magnetic anomalies, *Earth and Plan. Sci. Lett.*, **11**, 10-17, 1971.

Kono, M., Rikitake two-disk dynamo and paleomagnetism, *Geophys. Res. Lett.*, **14**, 21-24, 1987.

Kovacheva, M., Summarized results of the archeomagnetic investigation of the geomag-

netic field variation for the last 8000 yr in south-eastern Europe, *Geophys. J. R. Astr. Soc.*, **61**, 57-64, 1980.

Laj, C., Kissel, C., Lefevre, I., Relative geomagnetic field intensity and reversals from Upper Miocene sections in Crete, *Earth Plan. Sci. Lett.*, **141**, 67-78, 1996.

Langel, R.A. and Estes, R.H., A geomagnetic field spectrum, *Geophys. Res. Lett.*, **9**, 250-253, 1982.

Lehman, B., Laj, C., Kissel, C., Mazaud, A., Paterne, M., and Labeyrie, L., Relative changes of the geomagnetic field intensity during the last 280 kyear from piston cores in the Acores area, *Phys. Earth Plan. Int.*, bf 93, 269-284, 1996.

Lock, J. and M.W. McElhinney, The Global Paleomagnetic Database: design, installation, and use with ORACLE, *Surveys in Geophysics*, **12**, 317-506, 1991.

Lund, S.P. and Banerjee, S.K., The paleomagnetic record of Late Quaternary secular variation from Anderson Pond, Tennessee, *Earth Plan. Sci. Lett.*, **72**, 219-237, 1985.

Lund, S.P., Liddicoat, J.C., Lajoie, K.R., Henyey, T.L., and Robinson, S.W., Paleomagnetic evidence for long-term (10^4 year) memory and periodic behavior in the earth's core dynamo process, *Geophys. Res. Lett.*, **15**, 1101-1104, 1988.

McFadden, P.L. and Merrill, R.T., History of the Earth's magnetic field and possible connections to core-mantle boundary processes, *J. Geophys. Res.*, **100**, 307-316, 1995.

McLeod, M.G., Signals and noise in magnetic observatory annual means: Mantle conductivity and jerks, *J. Geophys. Res.*, **97**, 17,261-17,290, 1992.

McLeod, M.G., Spatial and temporal power spectra of the geomagnetic field, *J. Geophys. Res.*, **101**, 2745-2763, 1996.

Meynadier, L., Valet, J.-P., Bassonot, F.C., Shackleton, N.J. and Guyodo, Y., Asymmetrical saw-tooth pattern of the geomagnetic field intensity from equatorial sediments in the Pacific and Indian oceans, *Earth Plan. Sci. Lett.*, **126**, 109-127, 1994.

Meynadier, L., Valet, J.-P., Weeks, R., Shackleton, N.J. and Hagee, V.L., Relative geomagnetic intensity of the field during the last 140 ka, *Earth Plan. Sci. Lett.*, **114**, 39-57, 1992.

- Pal, P.C. and Roberts, P.H., Long-term polarity stability and strength of the geomagnetic dipole, *Nature*, **331**, 702-705, 1988.
- Pelletier, J.D. and Turcotte, D.L., Scale-invariant topography and porosity variations in sedimentary basins, *J. Geophys. Res.*, **101**, 28,165-28,175, 1996.
- Press, W.H., Teukolsky, S.A., Vetterling, W.T. and Flannery B.P., *Numerical Recipes in C: The Art of Scientific Computing*, second ed., Cambridge University Press, Cambridge, 1992.
- Seki, M. and Ito, K., A phase-transition model for geomagnetic polarity reversals, *J. Geomag. Geoelectr.*, **45**, 79-88, 1993.
- Stevenson, D.J., Planetary magnetic fields, *Rep. Prog. Phys.*, **46**, 555-620, 1983.
- Tauxe, L. and Hartl, P., 11 million years of Oligocene geomagnetic field behavior, *Geophys. J. Int.*, **128**, 217-229, 1997.
- Thibaut, J., Pozzi, J.-P., Barthes, V., and Dubuisson, G., Continuous record of geomagnetic field intensity between 4.7 and 2.7 Ma from downhole measurements, *Earth Plan. Sci. Lett.*, **136**, 541-550, 1995.
- Thouveny, N., Creer, K.M., and Blunk, I., Extension of the Lac du Bouchet palaeomagnetic record over the last 120,000 years, *Earth Plan. Sci. Lett.*, **97**, 140-161, 1990.
- Turcotte, D.L., *Fractals and Chaos in Geology and Geophysics*, Cambridge Univ. Press, Cambridge, 1992.
- Turner, G.M. and Thompson, R., Lake sediment record of the geomagnetic secular variation in Britain during Holocene times, *Geophys. J. R. Astron. Soc.*, **65**, 703-725, 1981.
- Valet, J.-P. and Meynadier, L., Geomagnetic field intensity and reversals during the past four million years, *Nature*, **366**, 234-238, 1993.
- van der Ziel, A., On the noise spectra of semiconductor noise and of flicker effect, *Physica*, **16**, 359-375, 1950.
- Verosub, K.L., Mehringer, P.J., and Waterstraat, P., Holocene secular variation in western North America: paleomagnetic record from Fish Lake, Harney County, Oregon, *J. Geophys. Res.*, **91**, 3609-3623, 1986.

Vicsek, T., *Fractal Growth Phenomena*, World Sci., River Edge, N. J., 1992.

Voorhies, C.V. and Conrad, J., Accurate predictions of mean geomagnetic dipole excursion and reversal frequencies, mean paleomagnetic field intensity, and the radius of the Earth's core using McLeod's rule, *NASA Technical Memorandum 104634*, 1996.

Weissman, M.B., $1/f$ noise and other slow, nonexponential kinetics in condensed matter, *Rev. Mod. Phys.*, **60**, 537-571, 1988.

FIGURE CAPTIONS

Figure 1: Paleointensity of the virtual axial dipole moment (VADM) of the earth's magnetic field (with reversed polarity data given by negative values) inferred from sediment cores for the past 4 Ma from Meynadier (1994).

Figure 2: Power spectrum of the geomagnetic field intensity variations estimated with the use of the Lomb periodogram from sediment cores of Meynadier (1992) and Meynadier (1994) and archeomagnetic data from Kovacheva (1980). The power spectrum S is given as a function of frequency f for time scales of 100 a to 4 Ma.

Figure 3: Cumulative frequency-length distribution of the lengths of polarity intervals during the last 170 Ma from the time scale of Harland et al. (1990) (solid curve), Cande and Kent (1992a,1995) (dashed curve), and the Cande and Kent (1992a,1995) time scale from C1 to C13 with cryptochrons included (dashed and dotted line).

Figure 4: (a) A $1/f$ noise with a normal distribution with mean of $8.9 \times 10^{22} \text{Am}^2$ and standard deviation of $3.4 \times 10^{22} \text{Am}^2$ representing the geomagnetic field intensity (VADM) in one polarity state. (b) Binormal $1/f$ noise constructed from the normal $1/f$ noise of (a) as described in the text.

Figure 5: Cumulative frequency-length polarity interval distributions from the Harland et al. (1990) time scale and that of the binormal, $1/f$ noise model of intensity variations. The distribution from the Harland et al. (1990) time scale (dashed curve) was also given in Figure 4. The solid line represents the average cumulative distribution from the $1/f$ noise model. The dotted lines represent the minimum and maximum reversal length distributions for 20 numerical experiments, thereby representing 95% confidence intervals.

Figure 6: Cumulative frequency-length polarity interval distributions for the $1/f$ noise model of intensity variations (shown in the middle, also given in Figure 5) and for intensity variations with power spectra proportional to $f^{-0.8}$ and $f^{-1.2}$. This plot illustrates that the polarity length distribution is very sensitive to the form of the power spectrum, allowing us to conclude that the agreement between the model and the observed distribution in Figure

5 is unique to $1/f$ noise intensity variations.

Figure 7: Pair correlation function of the reversal history according to the Harland et al. (1990) time scale (filled circles), Cande and Kent (1992a,1995) (unfilled circles), synthetic reversals produced from $1/f$ noise model of intensity variations (boxes), and a Poisson process (triangles). The real and synthetic reversals exhibit similar non-random clustering.

Figure 8: Power spectra of inclination and declination from the Lac du Bouchet sediment core. The declination spectrum is offset from the inclination spectrum so that they may be placed on the same graph.

Figure 9: Power spectra of inclination from the following locations, top to bottom: 1) Anderson Pond, 2) Bessette Creek, 3) Fish Lake, 4) Lake Bullenmerri, and 5) Lake Keilambete. The spectra are offset to place them on the same graph.

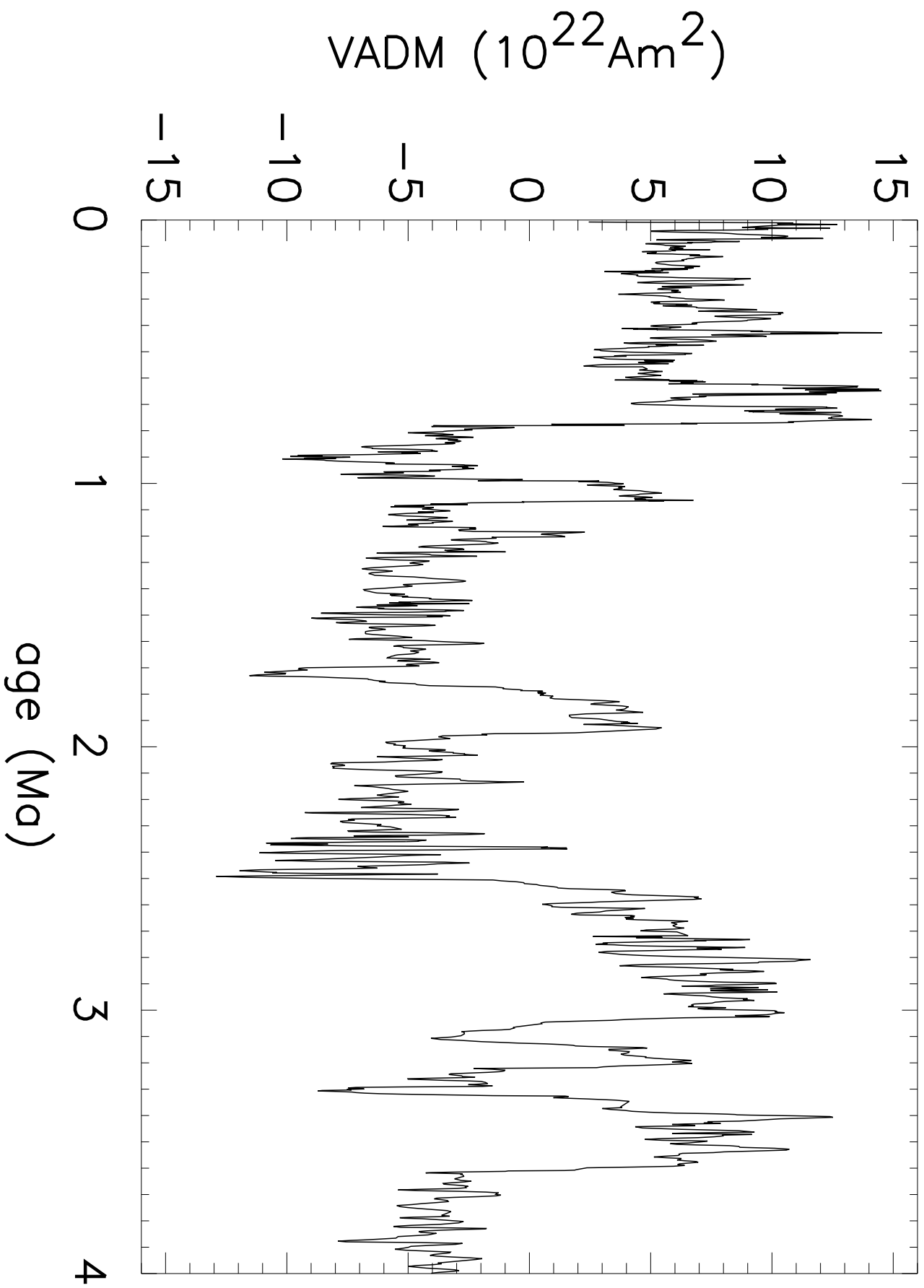
Figure 10: Dipole moment produced by the model normalized to the average dipole moment, set to be one. The field exhibits reversals with a broad distribution of polarity interval lengths and a variable reversal rate decreasing at later times in the simulation.

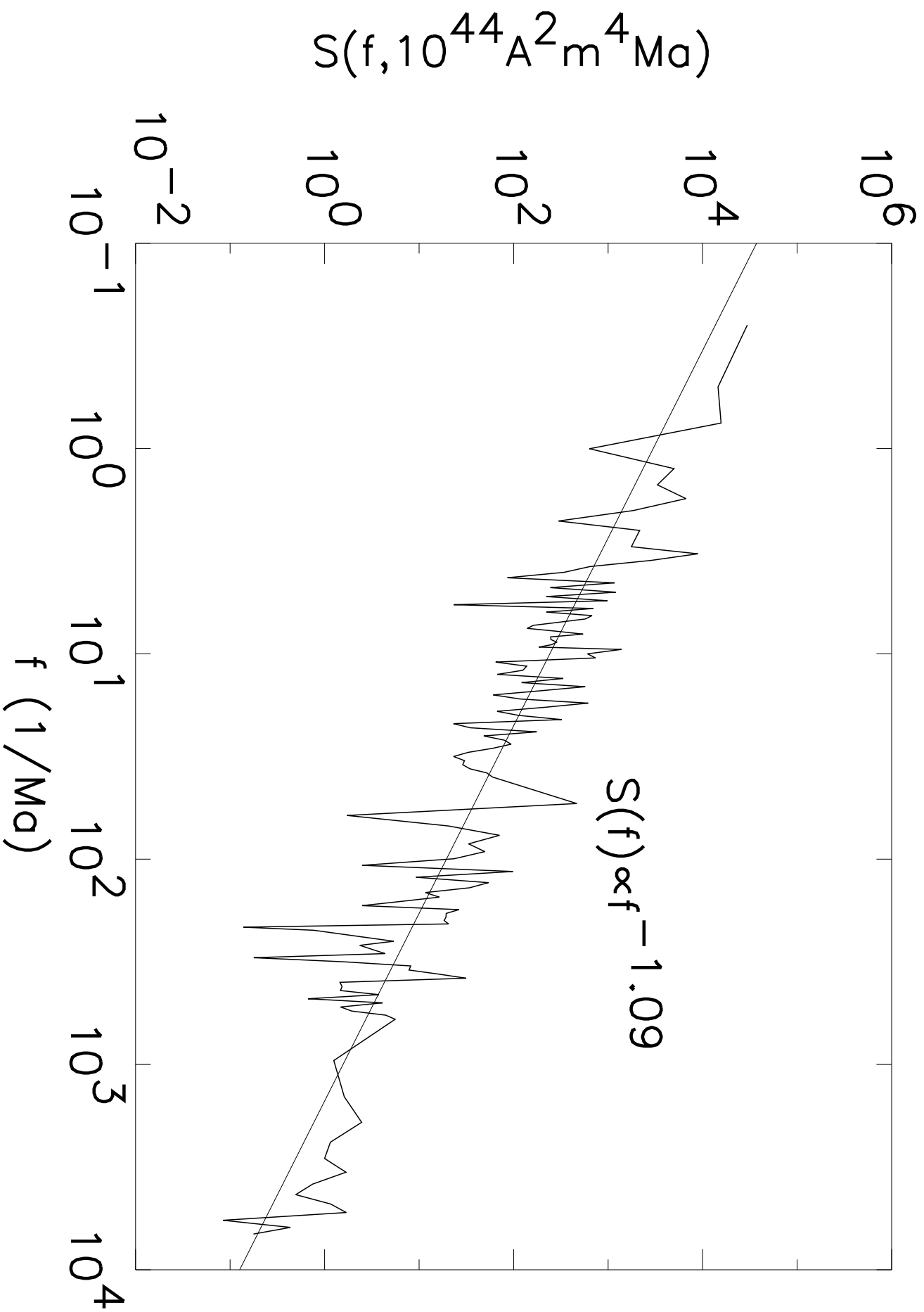
Figure 11: Distribution of magnetic field according to the ten simulations of the model (solid curve) and a binormal distribution fit to the data (dashed line). The binormal distribution fits the data well.

Figure 12: Average power spectrum of the mean value of the magnetic field (dipole field) from 25 simulations. The spectrum has a low-frequency spectrum with $S(f) \propto f^{-1}$ and a high frequency region $S(f) \propto f^{-2}$. The same spectrum is observed in geomagnetic intensity from sediment cores and historical data.

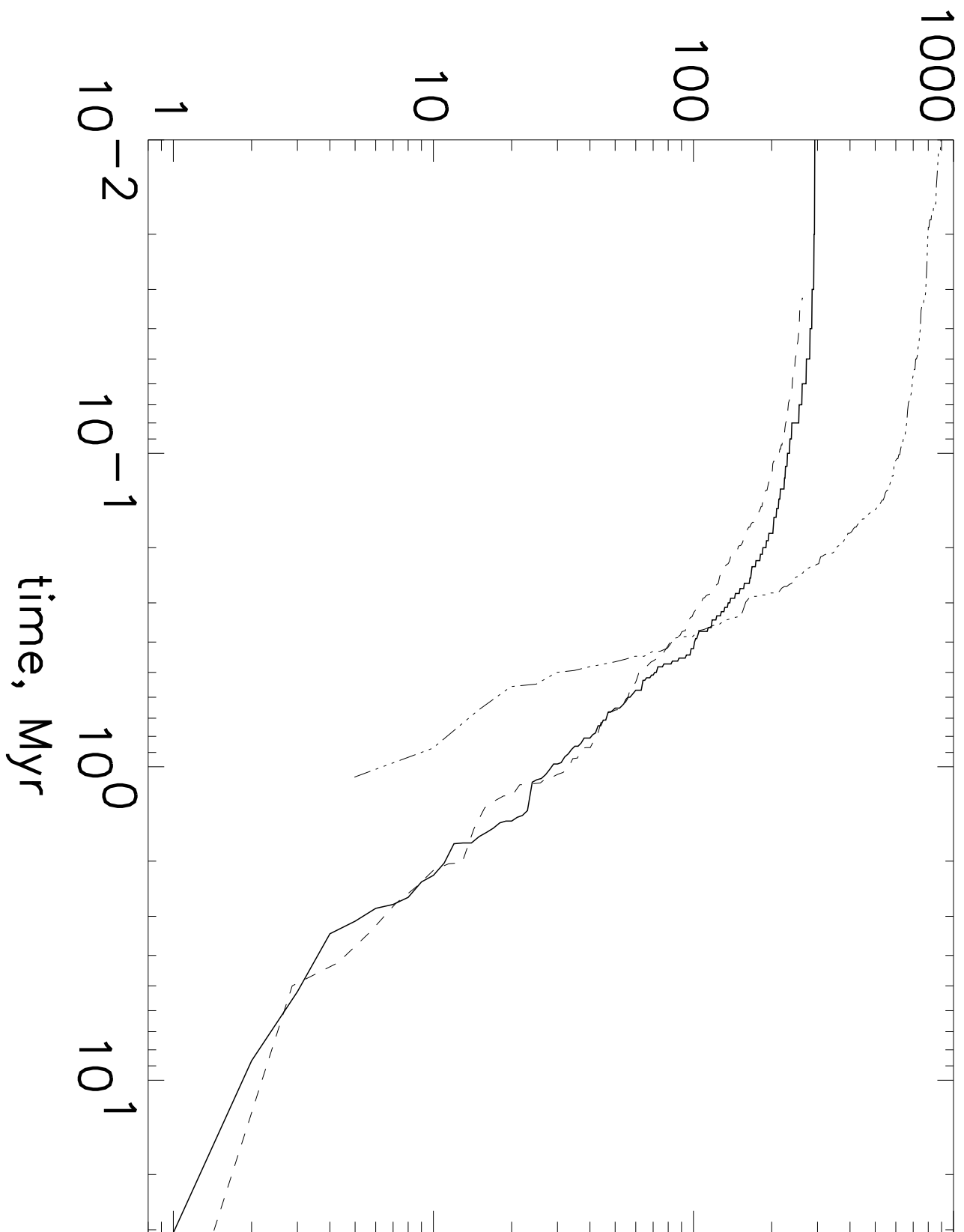
Figure 13: Average power spectrum of the angular deviation from a dipole field from 25 simulations. The spectrum is $S(f) \propto f^{-2}$ for high frequencies and gradually flattens out to a constant spectrum at low frequencies.

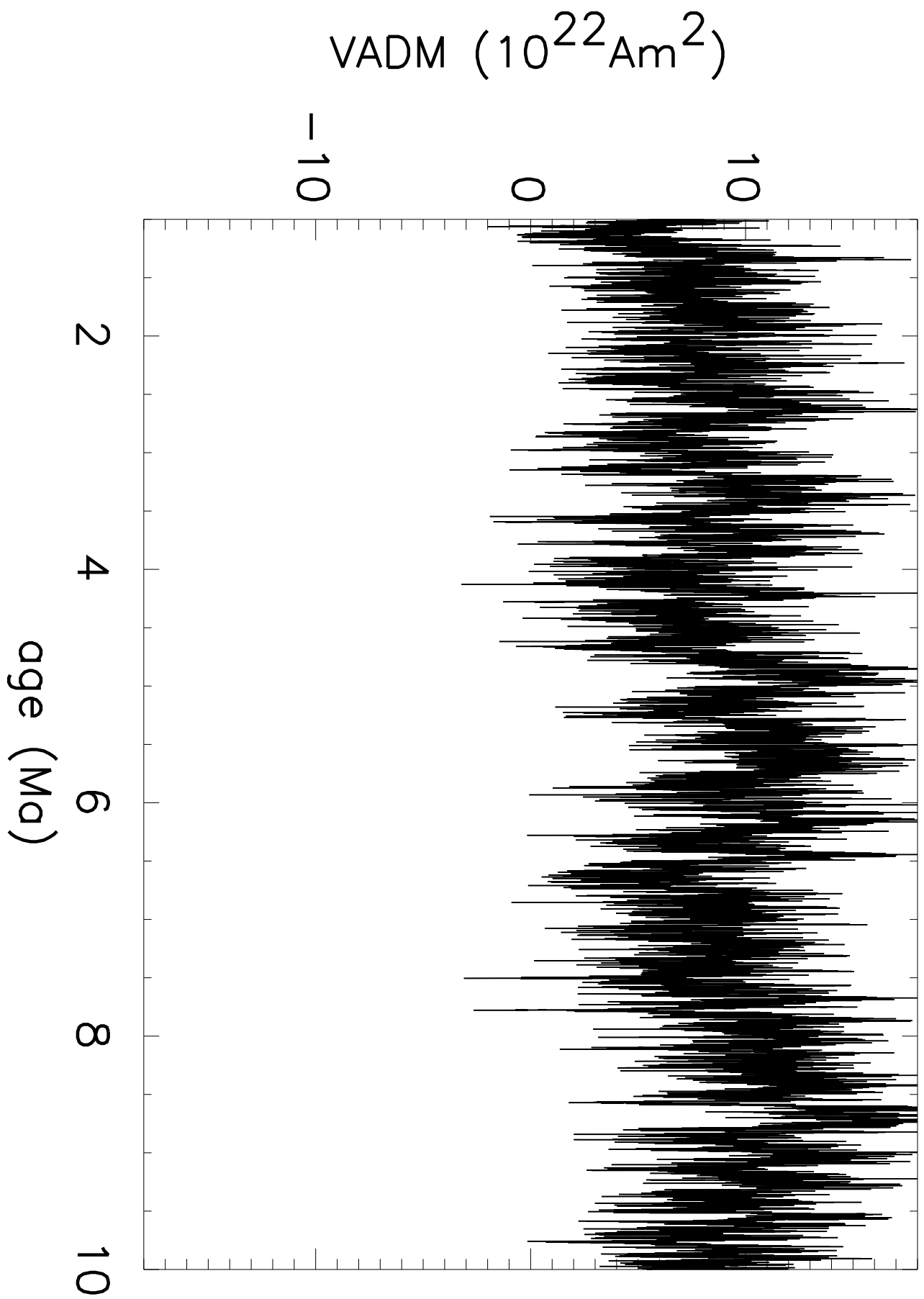
Figure 14: Average spatial power spectrum of transects of the magnetic field B_z . The power spectrum is $S(k) \propto k^{-1}$. This is precisely analogous to the power-law spectrum $R_n \propto n^{-1}$.

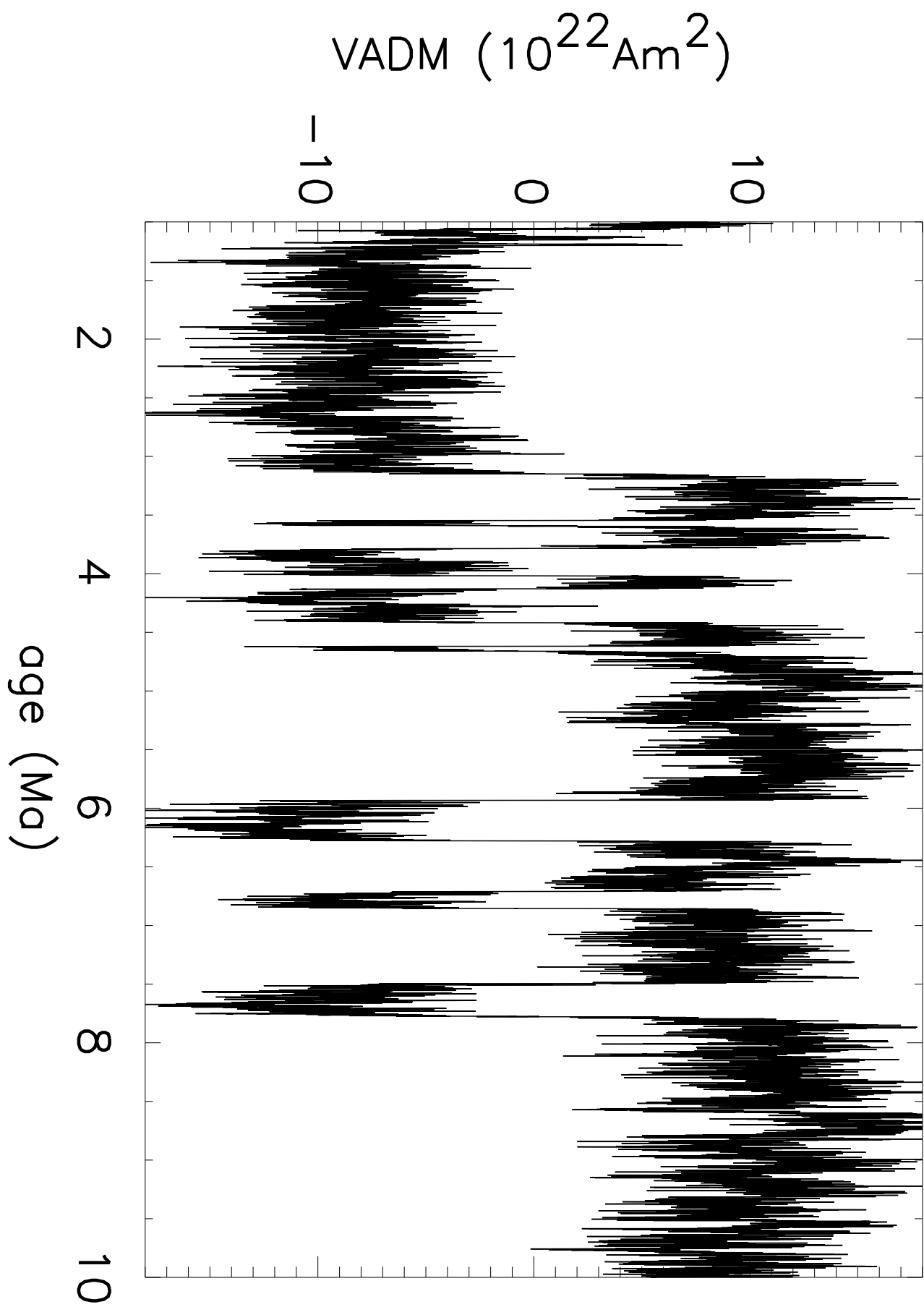




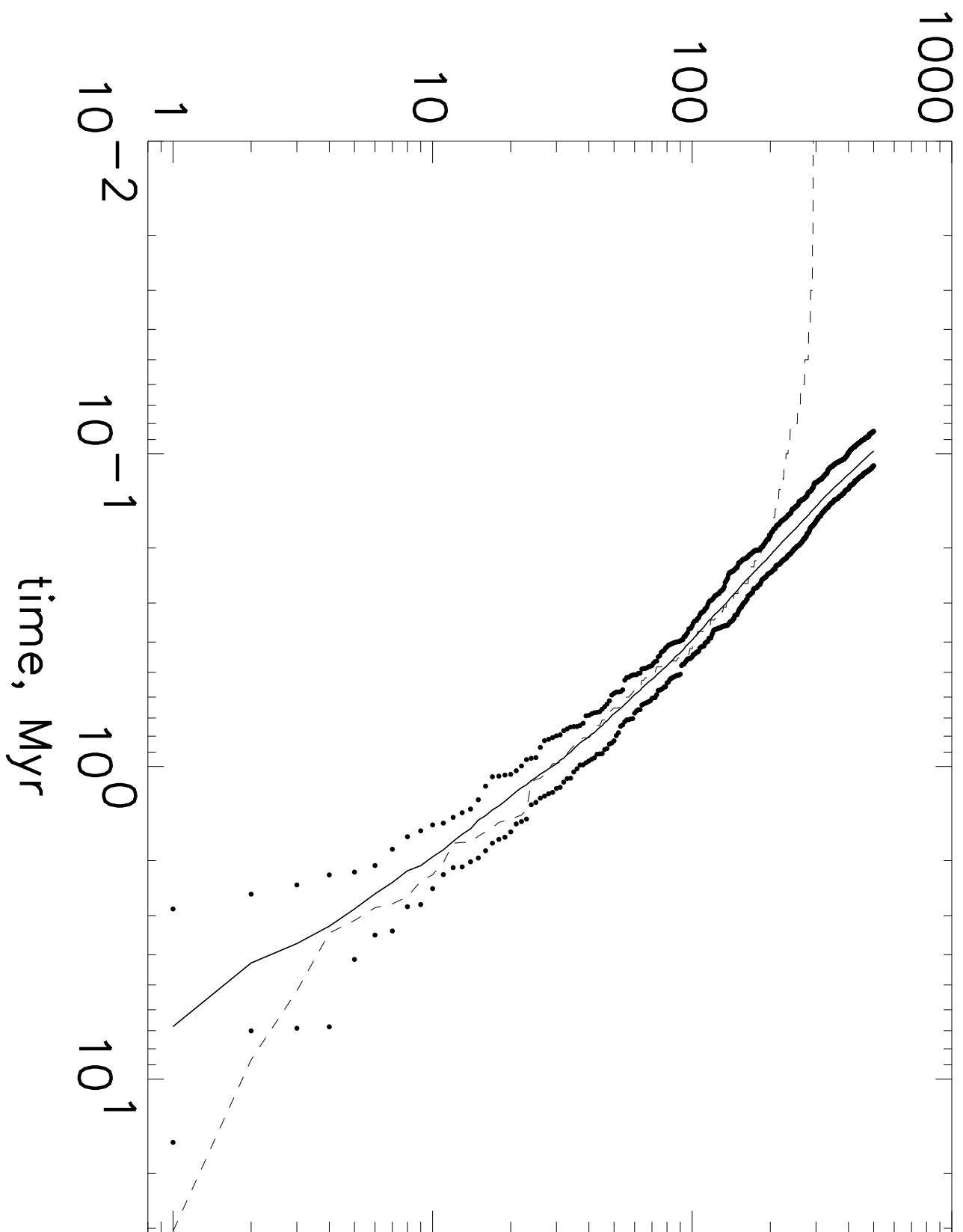
intervals > time

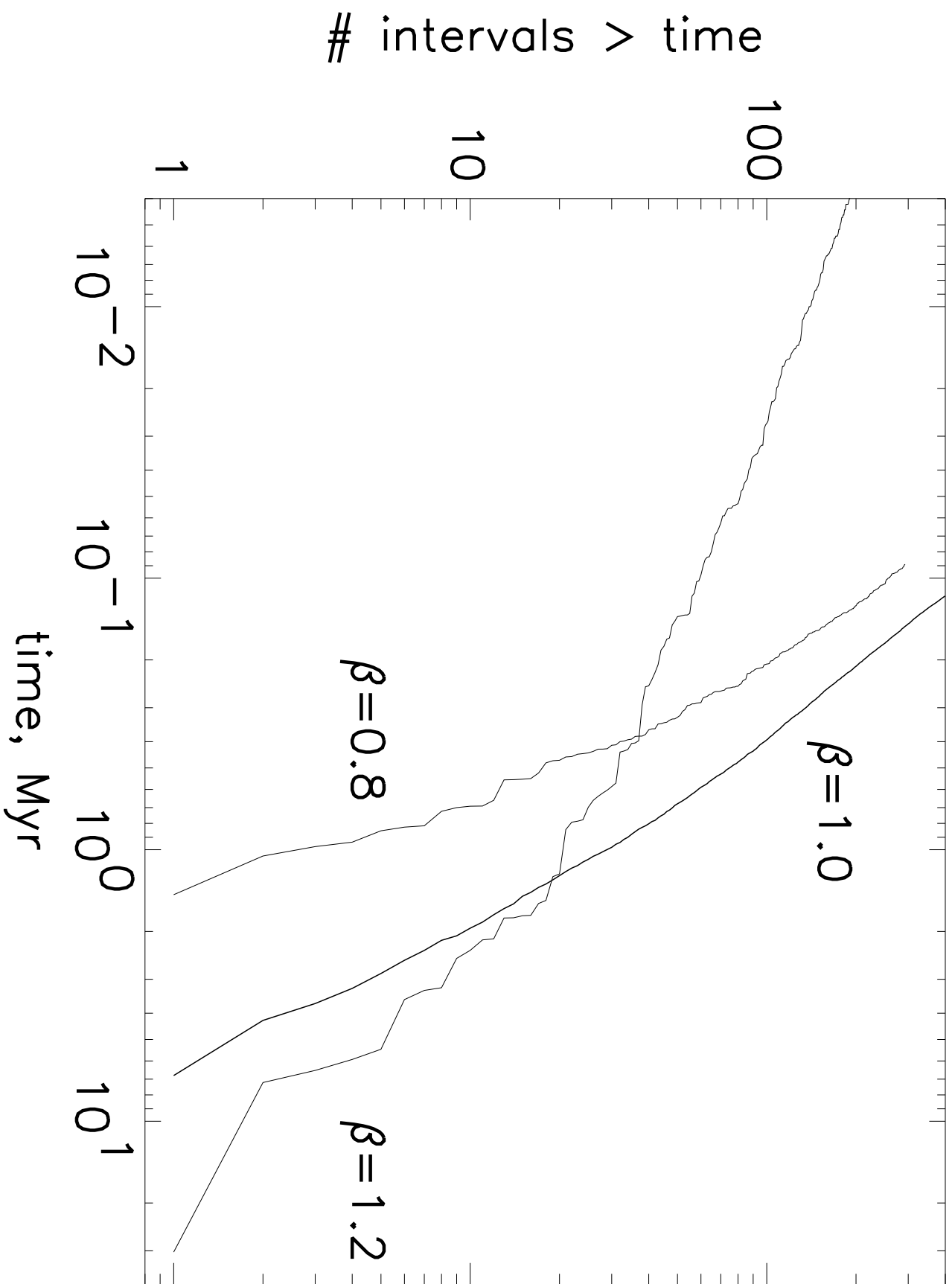


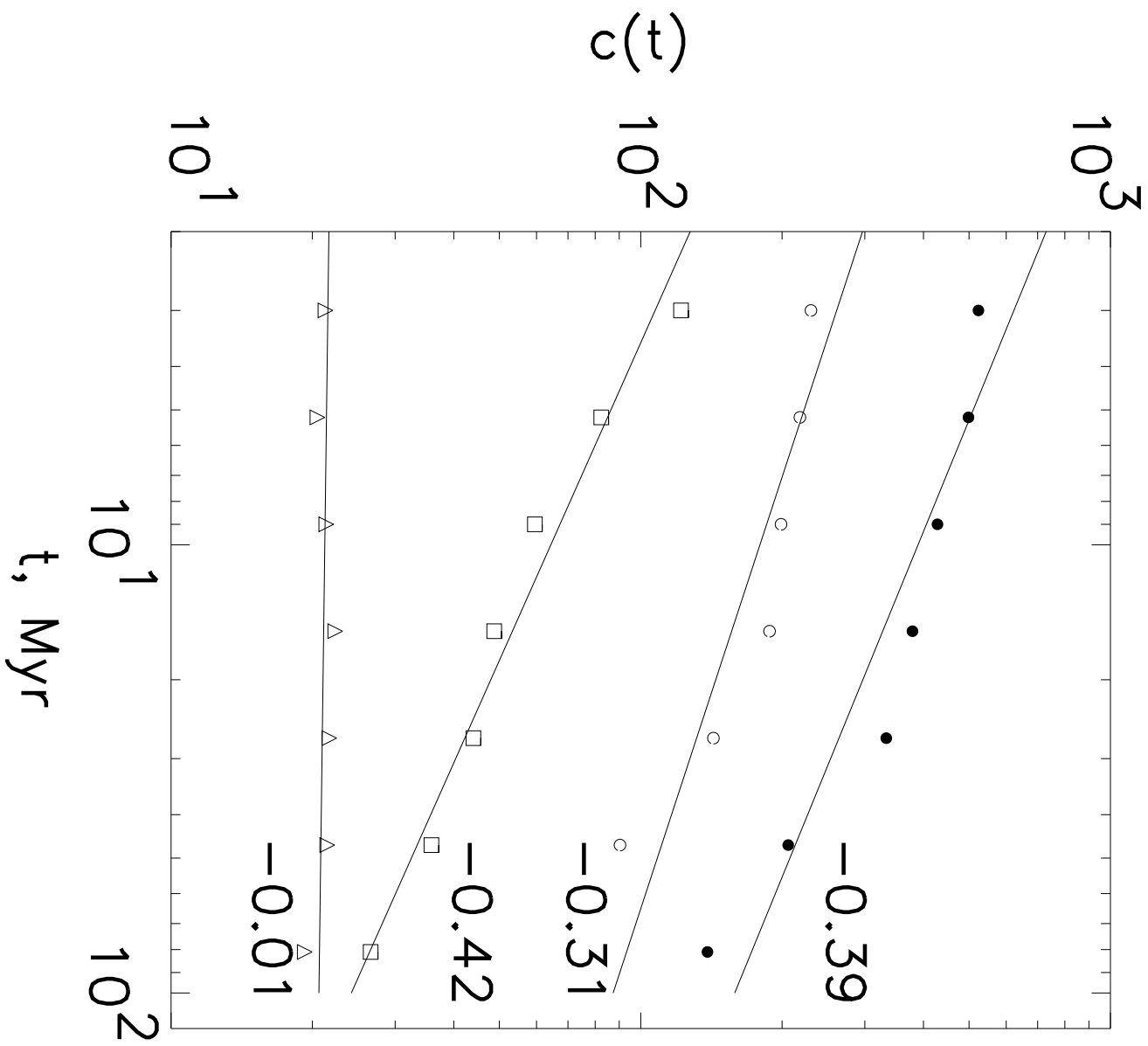


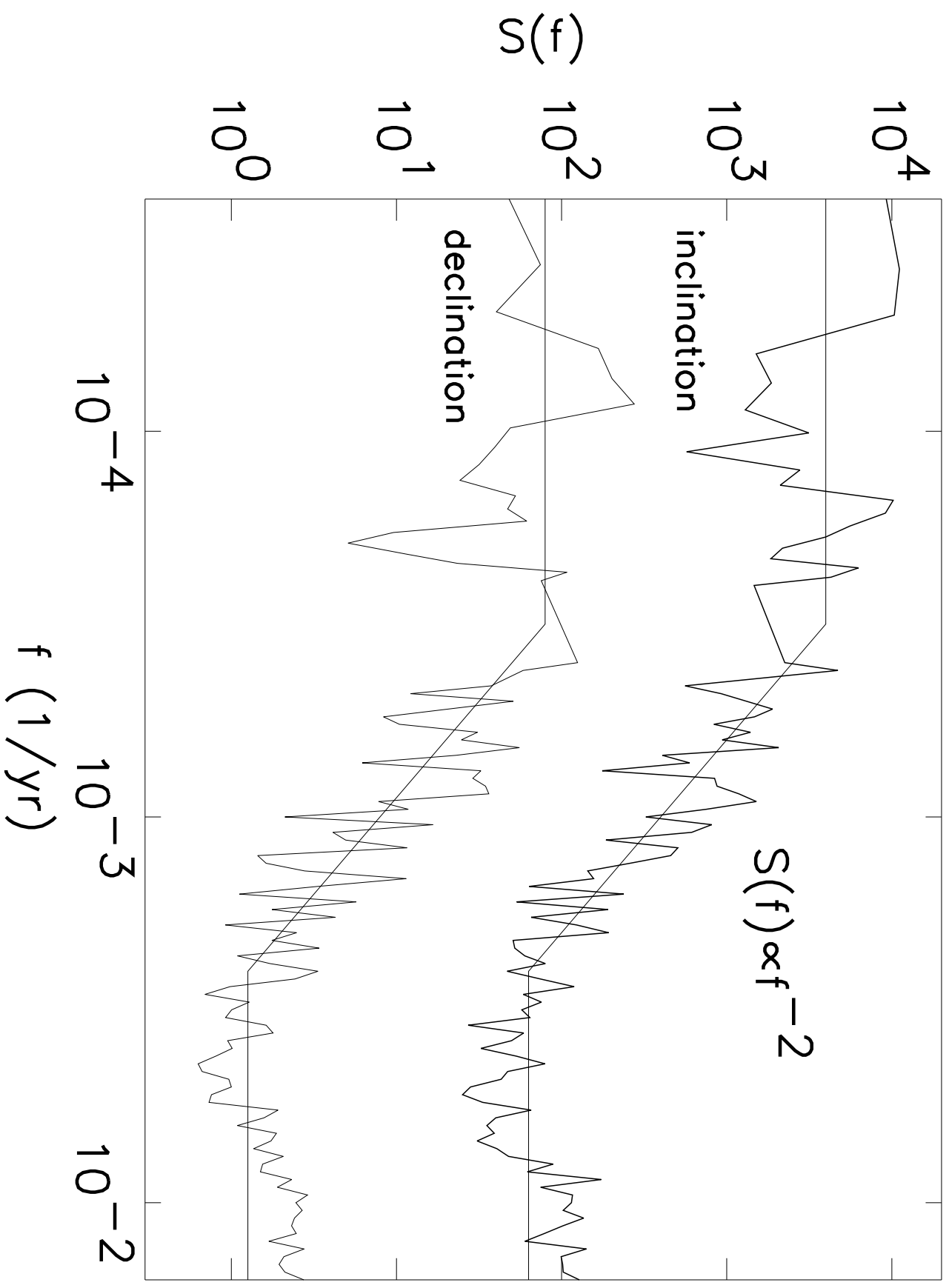


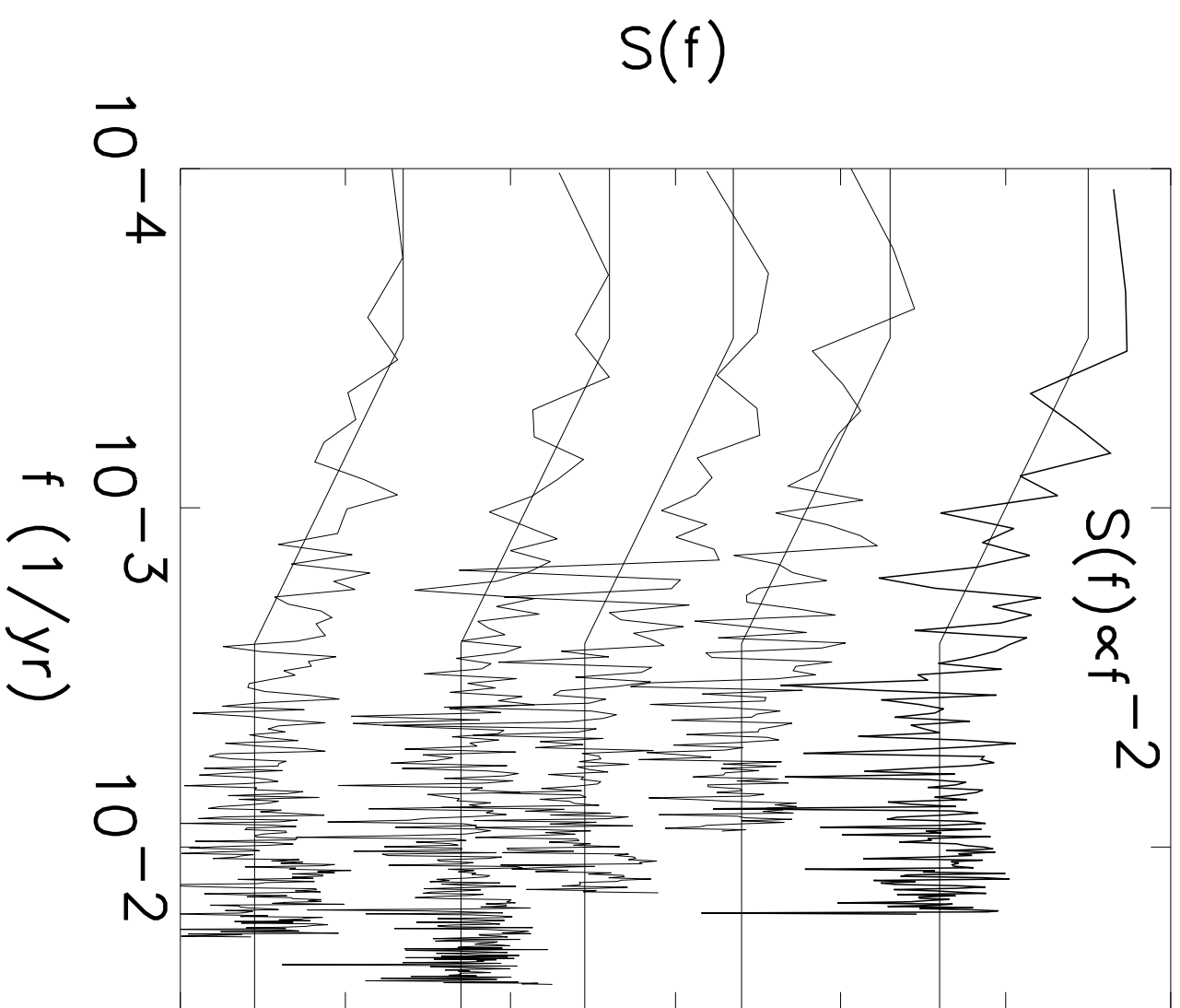
intervals > time

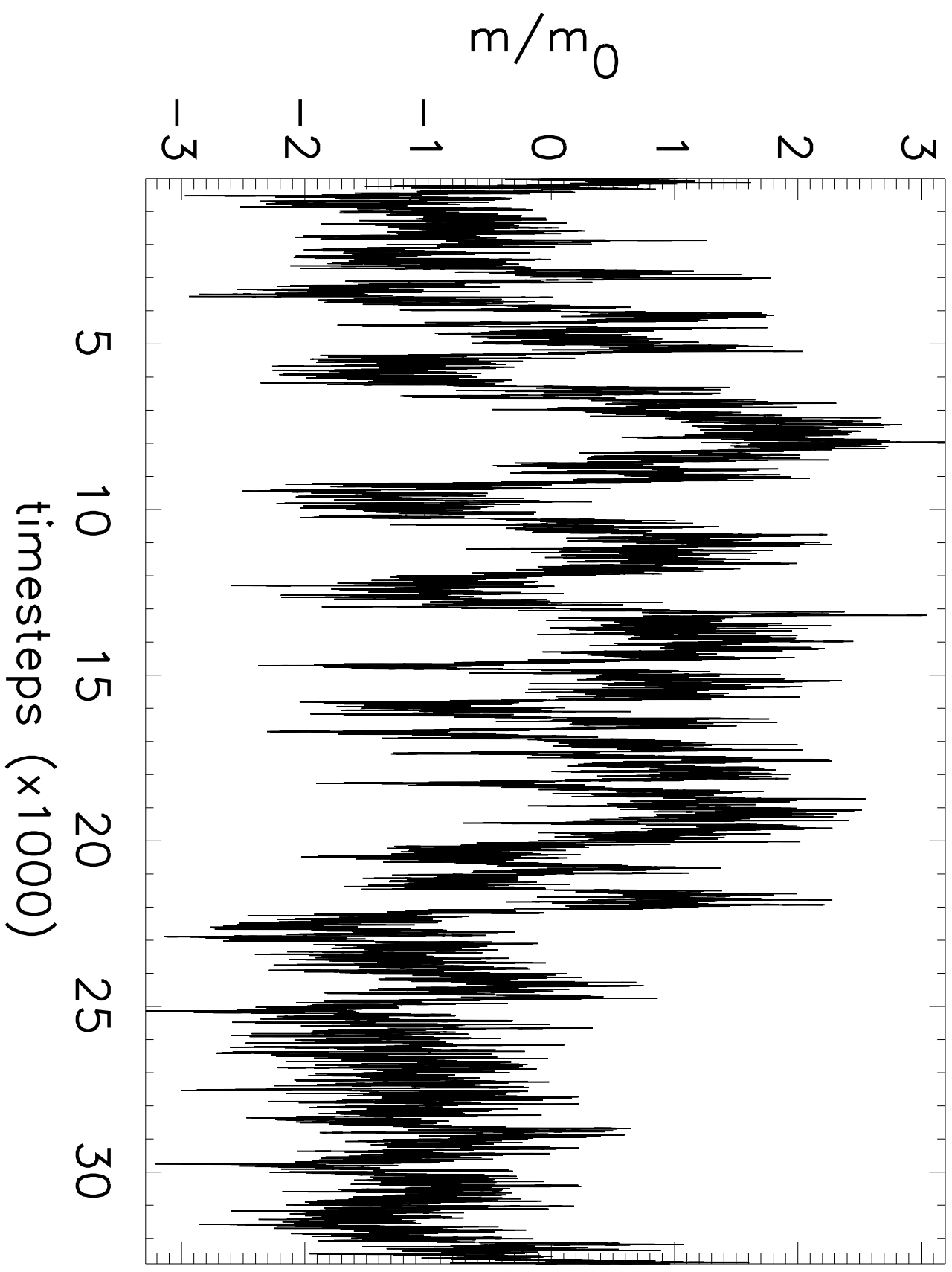












probability density function

